A Simple Method for Determining Kinetic Parameters for Materials in Fire Models

RICHARD E. LYON[1], NATALLIA SAFRONAVA[2], and EZGI OZTEKIN[2]
[1]Federal Aviation Administration
William J. Hughes Technical Center
Atlantic City International Airport, NJ 08405 USA
[2]Technology and Management International
Toms River, NJ USA

ABSTRACT

A semi-exact solution of the Arrhenius temperature integral is the basis for a new method to determine the effective activation energy E_a and frequency factor A for a first-order thermal decomposition process from the maximum mass loss rate m'_{max} and the temperature at maximum mass loss rate T_p recorded during a single thermogravimetric analysis experiment at constant heating rate. Results for kinetic parameters determined by the single-point (m'_{max}, T_p) method are compared to kinetic parameters determined by other non-isothermal analysis methods.

KEYWORDS: kinetics, thermal decomposition, modeling, TGA.

INTRODUCTION

The limitations of nonisothermal methods of thermal analysis include the choice of a particular reaction order for the kinetic analysis, the error associated with predicting rates outside the experimental range of heating rates, and the inability to derive mechanistic information [1]. However, for an inherently nonisothermal process such as fuel generation by a thermally decomposing polymer at a burning surface a simple kinetic model usually suffices for use in fire models [2]. Detailed mechanistic information may not be required for fire models because it is the rate of heat generation due to combustion of the chemical species, the completeness of this process, and the temperatures over which fuel generation occurs, not the chemical species themselves that are of primary interest [3].

APPROACH

The fuel generation rate of a material element in a burning solid is assumed to be equal to the change in mass m of the element per unit time t. For a first order thermal decomposition process with rate constant k and equilibrium char or inert mass m_c the mass loss rate is

$$-\frac{dm}{dt} = k(m - m_c) \tag{1}$$

A more convenient form of Eq. 2 for thermal analysis is obtained when the instantaneous mass is referenced to the initial sample mass, $m(0) = m_0$. Defining an instantaneous mass fraction $x(t) = x = m(t)/m_0$ and an equilibrium mass fraction, $x(\infty) = \mu = m_c/m_0$

$$-\frac{dx}{dt} = x' = k(x - \mu) \tag{2}$$

If k is of the Arrhenius form, $k = A\exp[-E_a/RT]$, Eq. 2 provides the relationship between the frequency factor A, activation energy E_a, universal gas constant R and the residual mass fraction at temperature T

$$\ln\left[\frac{x'}{x-\mu}\right] = \ln k \equiv \ln A - \frac{E_a}{RT}. \tag{3}$$

FIRE SAFETY SCIENCE-PROCEEDINGS OF THE TENTH INTERNATIONAL SYMPOSIUM, pp. 765-778
 / DOI: 10.3801/IAFSS.FSS.10-765

Equation 3 is the basis for the instantaneous rate method (IRM) by which A and E_a are determined from the intercept and slope of a plot of $\ln[x'/(x-\mu)]$ versus $1/T$ in an isothermal or temperature scanning (non-isothermal) experiment. A second method of kinetic analysis follows from the integrated form of Eq. 2

$$-\ln\left[\frac{x(t)-\mu}{1-\mu}\right]=\int_0^t A\exp\left[-\frac{E_a}{RT}\right]d\xi. \qquad (4)$$

A constant heating rate $\beta = dT/dt$ transforms the independent variable from time to temperature in Eq. 4, in which case the indefinite Arrhenius temperature interval has a semi-exact form for $E_a >> RT$ [4]

$$y=\frac{A}{\beta}\int_{T_0}^{T}\exp\left[-\frac{E_a}{R\theta}\right]d\theta \;\approx\; \frac{A}{\beta}\frac{R\theta^2 e^{-E_a/R\theta}}{(E_a+2R\theta)}\Bigg|_{T_0}^{T} \;\approx\; \frac{A}{\beta}\frac{RT^2 e^{-E_a/RT}}{(E_a+2RT)} \qquad (5)$$

The solution of Eq. 2 for the mass fraction $x(T)$ at temperature T in a temperature scanning experiment at constant heating rate for a first-order reaction is therefore

$$x(T)=\mu+(1-\mu)e^{-y} \qquad (6)$$

Differentiating Eq. 6 with respect to time at constant heating rate gives the specific mass loss rate $x'(T)$ at temperature T

$$x'(T)=-\frac{dx}{dt}=(1-\mu)ke^{-y} \qquad (7)$$

Setting the time derivative of Eq. 7 (second derivative of x with respect to time) equal to zero shows that the Arrhenius rate constant k has a particular value at the temperature of maximum pyrolysis rate, T_p [3]

$$k(T_p)=Ae^{-E_a/RT_p}=\frac{\beta E_a}{RT_p^2} \qquad (8)$$

The temperature at maximum pyrolysis rate T_p at heating rate β is obtained from A and E_a as the root $\lambda = E_a/RT_p$ of Eq. 8 written in the form

$$\ln\lambda^2+\lambda+\ln\left[\frac{\beta R}{AE_a}\right]=0 \qquad (9)$$

Substituting $k(T_p)$ into Eq. 7 gives the maximum fractional mass loss rate in a constant heating rate experiment,

$$x'_{\max}=x'(T_p)=(1-\mu)\frac{\beta E_a}{e^{\gamma}RT_p^2}\approx(1-\mu)\frac{\beta E_a}{eRT_p^2} \qquad (10)$$

The exponent γ in Eq. 10 is approximately equal to unity for typical polymer thermal decomposition parameters, $E_a >> 2RT_p$

$$\gamma=\frac{E_a}{E_a+2RT_p}\approx 1$$

Rearranging Eq. 10 gives E_a in terms of the quantities $x'_{\max}$, μ and T_p measured in a single thermogravimetric analysis (TGA) experiment at heating rate β

$$E_a = \frac{x'_{\max}}{1-\mu}\frac{eRT_p^2}{\beta} \tag{11}$$

If the constant heating rate thermal analysis experiment is conducted in a microscale combustion calorimeter [5] in which the anaerobic pyrolysis gases have heat of combustion h_c (J/g-gas) and are completely combusted in a separate oxidative process, the maximum heat release rate per unit initial mass of sample is $Q'(T_p) = Q'_{\max} = h_c x'_{\max}$. The total heat of combustion of the pyrolysis gases per unit initial mass of sample is $Q(T_\infty) = Q_\infty = h_c(1-\mu)$, and the equation for E_a in terms of the quantities measured in a microscale combustion calorimeter (MCC) is:

$$E_a = \frac{Q'_{\max}}{Q_\infty}\frac{eRT_p^2}{\beta} \tag{12}$$

The frequency factor is obtained from Eqs. 8 and 10 in terms of these same quantities

$$A = \frac{\beta E_a}{RT_p^2} e^{E_a/RT_p} = e\frac{x'_{\max}}{1-\mu} e^{E_a/RT_p} \tag{13}$$

$$A = e\frac{Q'_{\max}}{Q_\infty} e^{E_a/RT_p} \tag{14}$$

Equations 11, 12 and 13, 14 are the basis of the single-point method (SPM) for determining Arrhenius kinetic parameters from a single point ($x'_{\max}$, T_p) in TGA, or ($Q'_{\max}$, T_p) in MCC, at constant heating rate β in which μ or Q_∞ is measured after the test.

Equations similar to Eqs. 11-14 have been proposed [6,7] for determining the Arrhenius kinetic parameters for a reaction of arbitrary order *n*. In this method, which the authors refer to as the peak property method (PPM), the effective kinetic parameters E_a, A and n are determined by an iterative procedure that requires numerical evaluation of the Arrhenius integral in Eq. 5 between the limits T_0 and T_p for each increment of E_a, A and n until satisfactory agreement between the experiment and the analytic result for an *n*-th order reaction is obtained. The PPM is cumbersome because it neglects the semi-exact solution for the Arrhenius integral (last term in Eq. 5) and requires additional equations to determine the reaction order.

The advantage of the single-point, peak property, and instantaneous rate methods is the convenience of determining both kinetic parameters A and E_a from a single experiment. The disadvantage of these methods is that the kinetic parameters are measured at a single heating rate, rather that averaged over multiple heating rates as per the Kissenger method [8], so β should be in the range of interest.

The collection of terms RT_p^2/E_a appearing in Eqs. 8–12 has physical significance as the characteristic temperature interval for pyrolysis. This can be shown by writing the conservation of energy for a lumped system of small mass m having heat capacity c at temperature T

$$mc\frac{dT}{dt} = q_{in} - q_{out} \quad \text{(Watts)} \tag{15}$$

The left hand side of Eq. 15 is the rate of internal energy change of the sample resulting from the difference between the heat flow into and out of the sample during pyrolysis on the right hand side. For a temperature interval T-T_i over which heat is transferred into the sample by convection during pyrolysis $q_{in} = hS(T-T_i)$, where h and S are the overall heat transfer coefficient and surface area of the sample. The heat loss from the

sample due to thermal decomposition and vaporization of the pyrolysis products having heat h_{dec} (J/g) is $q_{out} = mh_{dec}A\exp[-E_a/RT]$. If $dT/dt = 0$ during pyrolysis for $T > T_i$ then $q_{in} = q_{out}$ and

$$hS(T - T_i) = mh_{dec}Ae^{-E_a/RT} \tag{16}$$

For small changes in q_{in} and q_{out} at temperatures in the vicinity of T_i Eq. 16 can be differentiated with respect to T

$$hS = mh_{dec}Ae^{-E_a/RT}\frac{E_a}{RT^2} \tag{17}$$

Dividing Eq. 17 by Eq. 16, for $T = T_p$

$$T_p - T_i = \frac{RT_p^2}{E_a} \tag{18}$$

Equation 18 shows that RT_p^2/E_a is the characteristic temperature interval of the pyrolysis reaction for a finite starting mass m having heat of decomposition h_{dec} in a constant heating rate thermal analysis experiment. This same reasoning and result applies if h_{dec} is a heat of melting or heat of chemical reaction measured in a differential scanning calorimeter. The significance of Eq. 18 with regard to fire behavior derives from empirical data [9] that show that the ignition temperature T_{ign} is a couple of pyrolysis intervals lower than T_i so approximately,

$$T_{ign} \approx T_p - \frac{eRT_p^2}{E_a} \tag{19}$$

EXPERIMENTAL

Materials

Samples of polymethylmethacrylate (PMMA), high impact polystyrene (HIPS), poly(hexamethylene adipamide) (PA66), polycarbonate of bisphenol-A (PC) and polyetherimide (PEI) were obtained from commercial sources as unmodified/natural resins and were tested as received. Gases were high purity (99.99 %) analytical grades obtained from Welco/CGI.

Thermal Analysis Methods

Mass loss rate in a temperature scanning experiment (nonisothermal conditions) was measured on a thermogravimetric analyzer (Mettler Toledo TGA/SDTA 851) under nitrogen at a flow rate of 20 cm^3/min at heating rates β = 3, 10, 30 and 60 K/min.

Numerical Methods

A one-dimensional pyrolysis model (ThermaKin) with chemical kinetics, heat and mass transfer, and in-depth absorption of radiant energy [10] was used to estimate the effective heating rate at the surface of a burning polymer in a standard fire calorimeter test [11].

RESULTS

Heating Rates at the Surface of Burning Polymers

Numerical evaluation of the heating rate at the surface during steady burning was performed using ThermaKin for a typical polymer [12] having kinetic parameters A = 1.9×10^{18} s^{-1}, E_a = 295 kJ/mol, thermal conductivity

κ = 0.24 W/m·K, density ρ = 1100 kg/m^3, heat of decomposition h_{dec} = 0.835 MJ/kg [13] and total heat of gasification $h_g = h_{dec} + c(T_p - T_i)$ = 2.30 MJ/kg over a range of external heat fluxes q''_{ext}. The heating rate at the surface was also calculated using the analytic solution [3] for a steadily-burning, semi-infinite slab of polymer having the same thermal and kinetic properties as were used in the ThermaKin calculation, with T_p calculated from the kinetic parameters and ThermaKin heating rate using Eq. 9.

$$\left.\frac{dT}{dt}\right|_{x=0} = \frac{q''^2_{net}}{\kappa\rho h_g}\left(1-\frac{h_{dec}}{h_g}\right) = \frac{\left(q''_{ext}-\sigma T_p^4\right)^2}{\kappa\rho h_g}\left(1-\frac{h_{dec}}{h_g}\right) \qquad (20)$$

The ThermaKin results in Table 1 are in general agreement with the analytic (Eq. 20) results as well as experimental data β = 3.0 ±0.5 K/s measured at the surface of PMMA during steady burning in a fire calorimeter at an external heat flux of 70 kW/m^2 [14]. Consequently, kinetic parameters obtained from thermal analyses at heating rates on the order of 1 K/s are directly applicable to fire models.

Table 1. Heating rates at a typical burning polymer surface.

External heat flux (kW/m^2)	**Heating rate (K/s)**	
	ThermaKin	**Eq. 20**
25	N/A	N/A
50	1.4	0.8
75	3.0	2.8
100	5.0	5.8

Comparison of Kinetic Models

Figure 1 is a graphical comparison of the specific mass loss rate calculated by Eq. 7 for μ = 0 with y obtained by numerical integration of the Arrhenius integral and the semi-exact solution (analytic result in Eq. 5) for a TGA experiment beginning at T = 300 K (25 °C) at a constant heating rate β = 10 K/min (0.167 K/s) for a material having $A = 2 \times 10^{20}$ s^{-1} and E_a = 301 kJ/mol. It is clear that the numerical and analytic solutions for y in Eq. 5 are indistinguishable when used in Eq. 7, so that E_a and A may be reliably obtained from the analytic solution after suitable manipulation (i.e., Eqs. 11 and 13).

Figure 2 shows TGA data for high impact polystyrene (HIPS) at β = 10 K/min and the first-order analytic approximation (Eq. 7) for $A = 2 \times 10^{20}$ s^{-1} and E_a = 301 kJ/mol determined by the single-point method (Eqs. 11 and 13) and μ = 0.03 measured after the test.

Table 2 contains kinetic parameters for PEI, PC, HIPS, PA66 and PMMA obtained by the single-point method (Eqs. 11 and 13), by the instantaneous rate method (Eq. 3) and by the Kissinger method [8]. Single point and instantaneous rate kinetic parameters are the average of individual values obtained at β = 3, 10, 30 and 60 K/min.

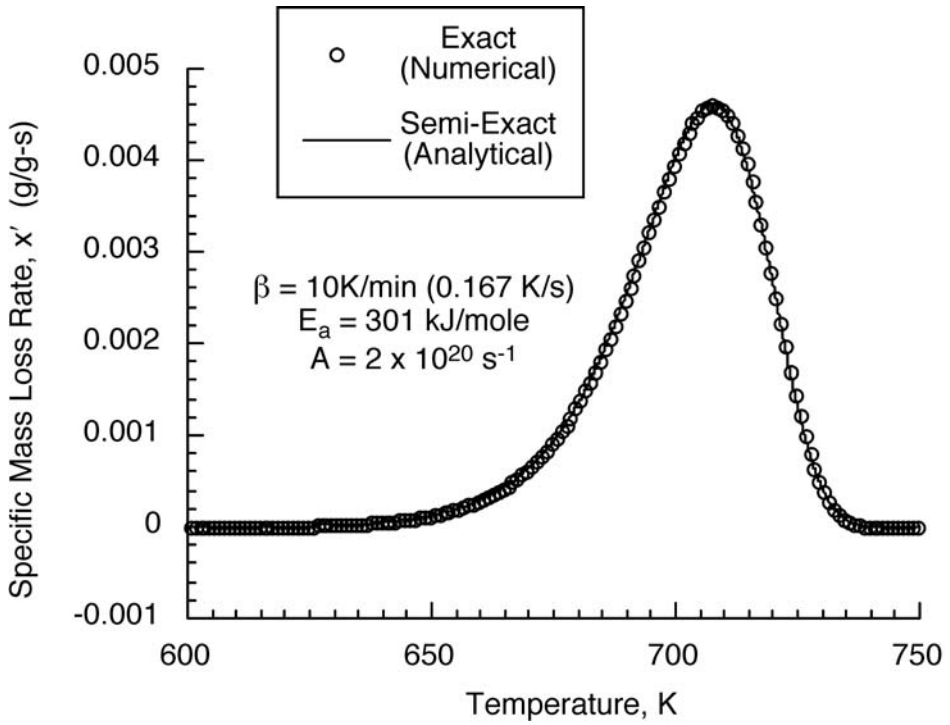

Fig. 1. Comparison of numerical solution of the Arrhenius temperature integral to the semi-exact/analytic approximation for a material with $A = 2 \times 10^{20}$ s^{-1}, $E_a = 301$ kJ/mol and $\mu = 0$ in a constant heating rate TGA experiment.

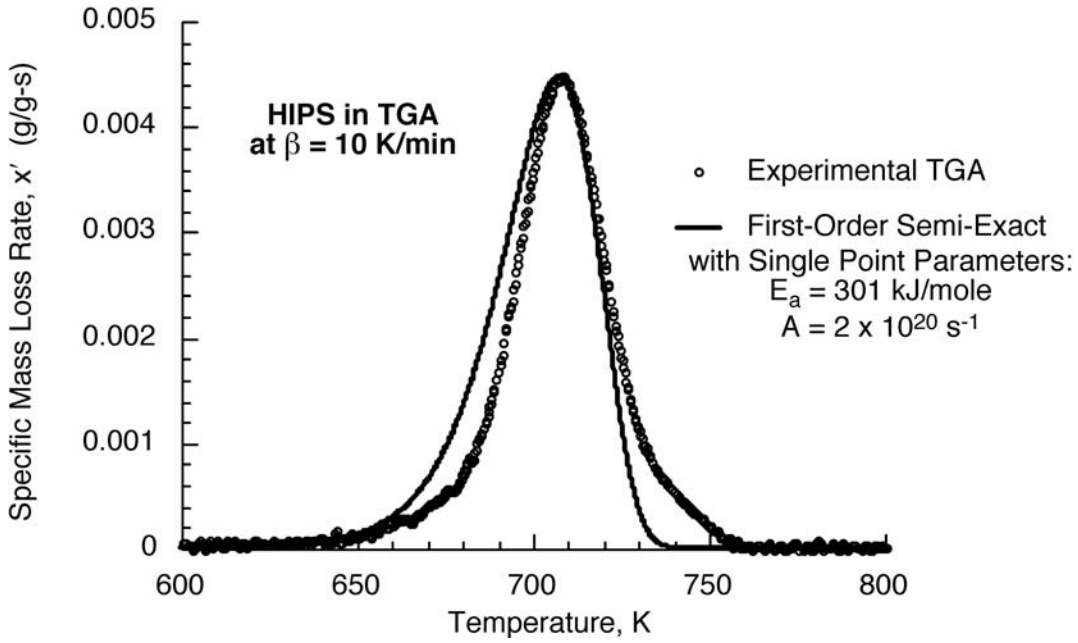

Fig. 2. TGA data in nitrogen for HIPS at $\beta = 10$ K/min compared to first-order analytic prediction using single point parameters $E_a = 301$ kJ/mol and $A = 2 \times 10^{20}$ s^{-1} obtained from TGA data Using Eqs. 11 and 13, respectively.

Table 2. First-order kinetic parameters obtained by three methods.

		Instantaneous rate (β average)		**Single point (β average)**		**Kissenger**	
Polymer	μ	E_a (kJ/mol)	ln A (s^{-1})	E_a (kJ/mol)	ln A (s^{-1})	E_a (kJ/mol)	ln A (s^{-1})
PMMA	0.00	223	36.33	213	34.88	237	39.48
HIPS	0.03	314	48.45	302	46.93	245	36.93
PA66	0.03	232	33.80	242	35.57	178	29.72
PC	0.24	397	55.12	428	60.13	254	33.74
PEI	0.54	418	56.43	370	50.09	234	29.72

Figure 3 is a plot of the TGA data for PMMA at β = 3, 10, 30 and 60 K/min (open circles) and the first order approximation using A and E_a determined for each heating rate by the instantaneous rate method (solid lines).

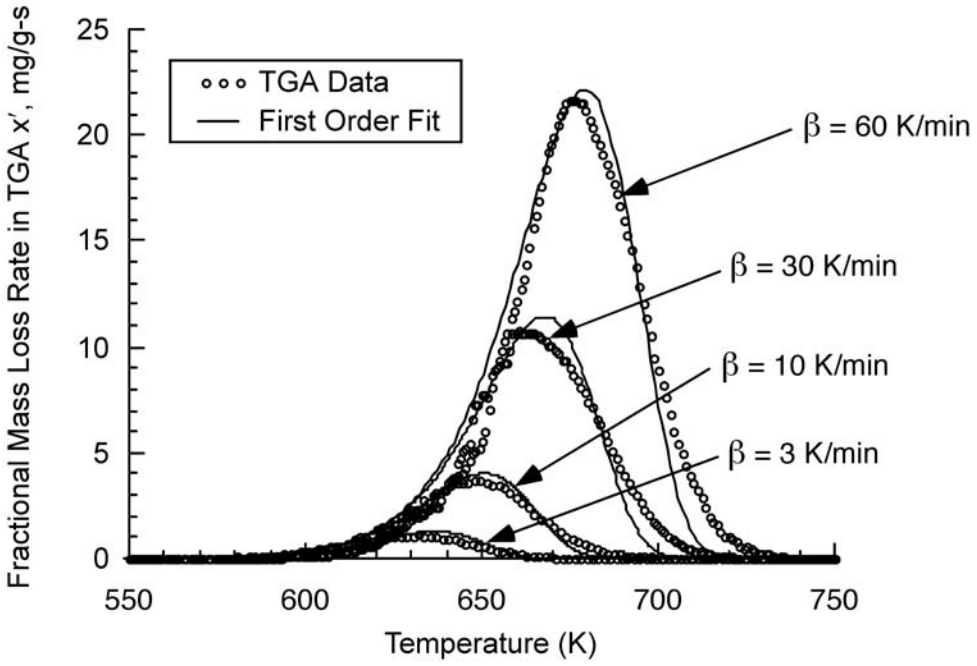

Fig. 3. TGA data for PMMA (open circles) and first-order approximation for A and E_a determined by the instantaneous rate method at each heating rate (solid lines).

Figure 4 is a plot of the TGA data for PMMA at β = 3, 10, 30 and 60 K/min and the first-order approximation with μ = 0 using A and E_a determined for each heating rate by the single point method.

Figure 5 is a plot of the TGA data for PMMA at β = 3, 10, 30 and 60 K/min and the first-order approximation with μ = 0 using A and E_a determined as average values over the range of heating rates by the Kissenger method [8].

Figure 6 is a plot of the TGA data for polycarbonate (PC) at β = 3, 10, 30 and 60 K/min and the first-order approximation with μ = 0.24 using A and E_a determined for each heating rate by the instantaneous rate method.

Figure 7 is a plot of the TGA data for polycarbonate (PC) at β = 3, 10, 30 and 60 K/min and the first-order approximation with μ = 0.24 using A and E_a determined for each heating rate by the single point method.

Figure 8 is a plot of the TGA data for polycarbonate(PC) at β = 3, 10, 30 and 60 K/min and the first-order approximation with μ = 0.24 using A and E_a determined as average values over the range of heating rates according to the Kissenger method [8].

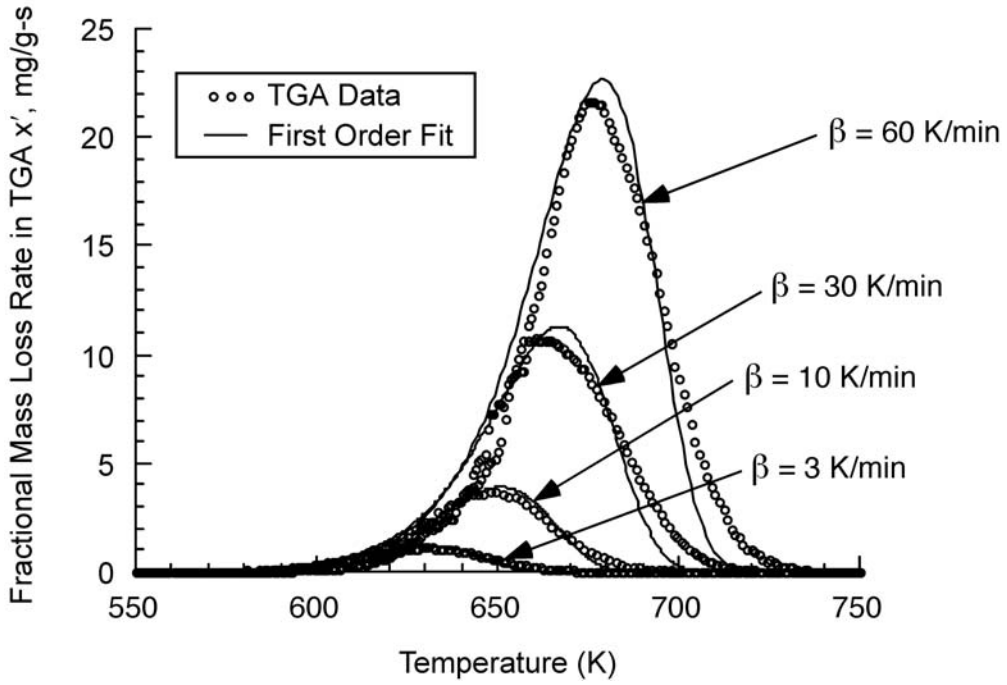

Fig. 4. TGA data for PMMA (open circles) and first-order approximation for A and E_a determined by the single point method at each heating rate (solid lines).

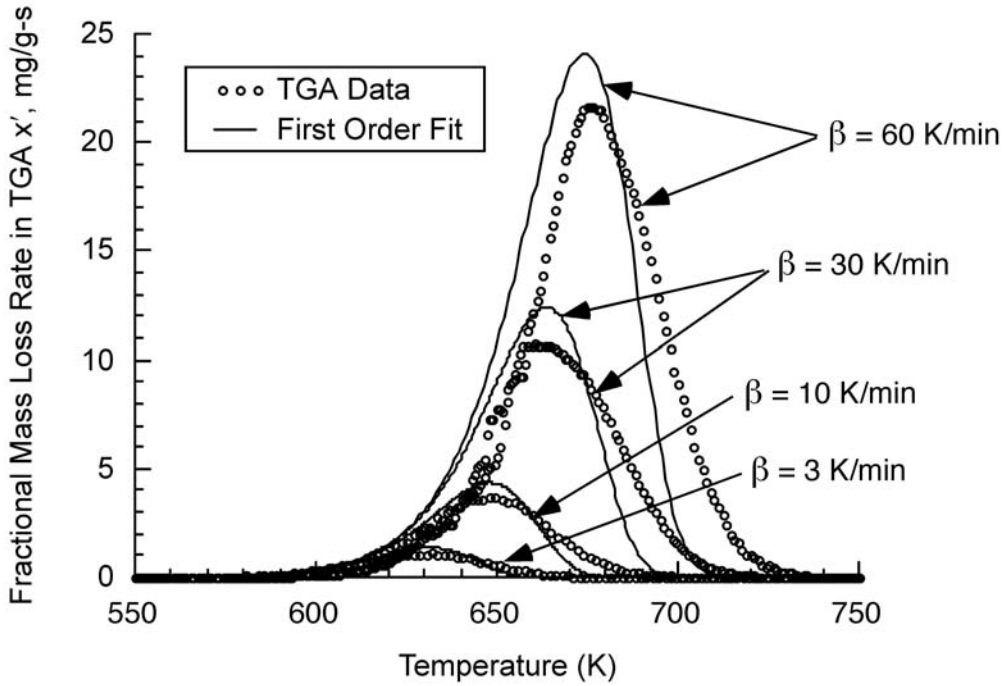

Fig. 5. TGA data for PMMA (open circles) and first-order approximation for A and E_a determined by the Kissenger method (solid lines).

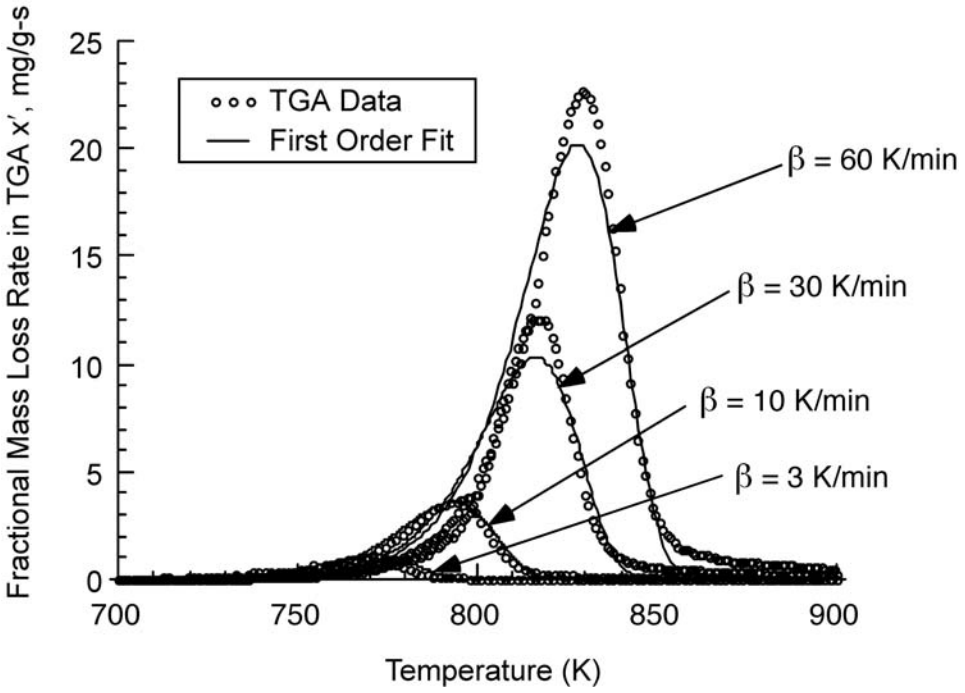

Fig. 6. TGA data for PC (open circles) and first-order approximation for A and E_a determined by the instantaneous rate method (solid lines).

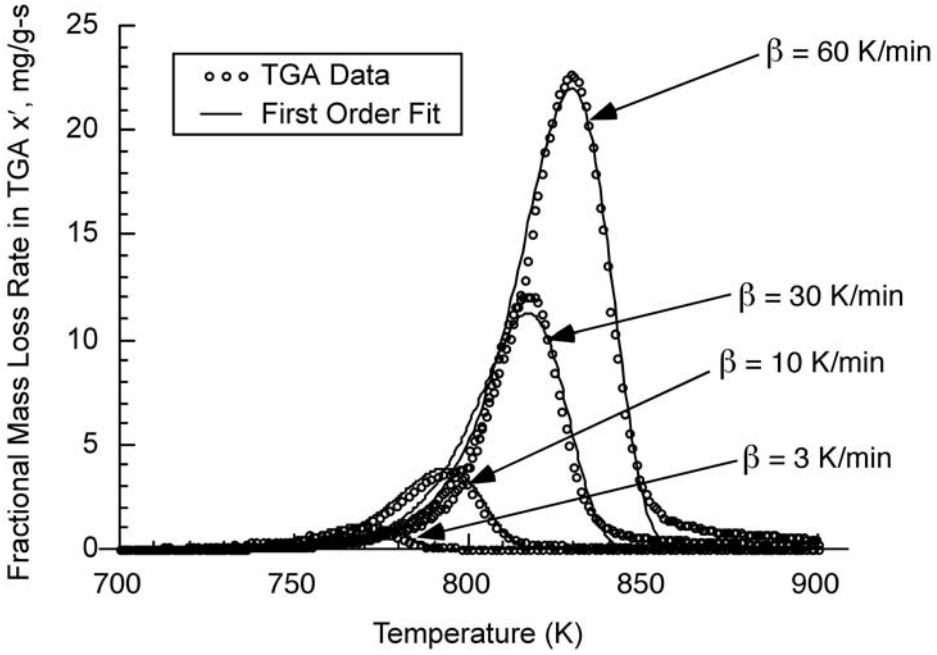

Fig. 7. TGA data for PC (open circles) and first-order approximation for A and E_a determined by the single point method at each individual heating rate (solid lines).

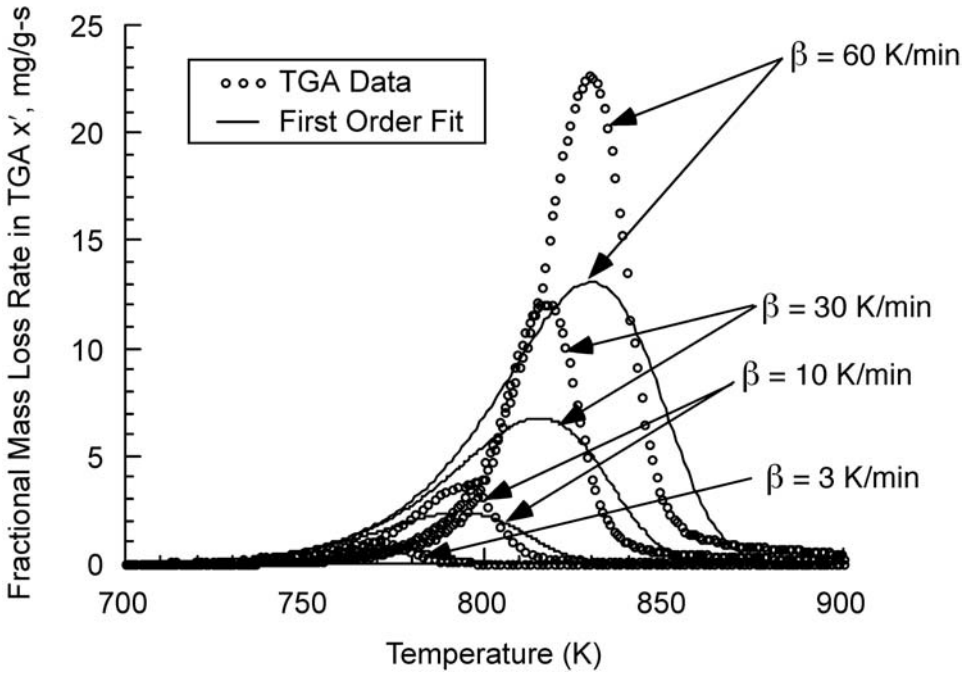

Fig. 8. TGA data for PC (open circles) and first-order approximation using A and E_a determined by the Kissenger method (solid lines) in Table 1.

It is clear from Figs. 3 through 8 that kinetic parameters determined at the heating rate of interest using the instantaneous rate or single point methods provide a better approximation to the experimental data in a first-order model than the kinetic parameters determined as average values over multiple heating rates (Kissenger method). The reason for the poor first-order approximation for PC using the Kissenger method parameters derives from the fact that the thermal decomposition process is not first-order as is evident from the instantaneous rate data in Fig. 9, which contains the plots of ln(k) on the left hand ordinate versus 1/T on the upper abscissa as well as the original data (lower right ordinate/abscissa) for each of the heating rates in this study. The upper and lower abscissas are coincident with respect to temperature to show the portion of the mass loss rate curve associated with each set of kinetic parameters. It is seen that the ln(k) vs. 1/T data is linear over a large portion of the fractional mass loss rate and that the slopes (E_a/R) are the same for all heating rates but the intercepts of these plots ln(A) are different for each heating rate.

Figure 10 shows TGA data for HIPS in an instantaneous rate plot as per Fig. 9. In contrast to Fig. 9 however, Fig. 10 shows that both the slopes and intercepts of the ln(k) versus 1/T plots are the same for the different heating rates, which implies that the HIPS thermal decomposition reaction is adequately described by first-order kinetics and this is the reason that the Arrhenius parameters in Table 2 are relatively consistent for HIPS as well as for PMMA and PA66 for the three methods.

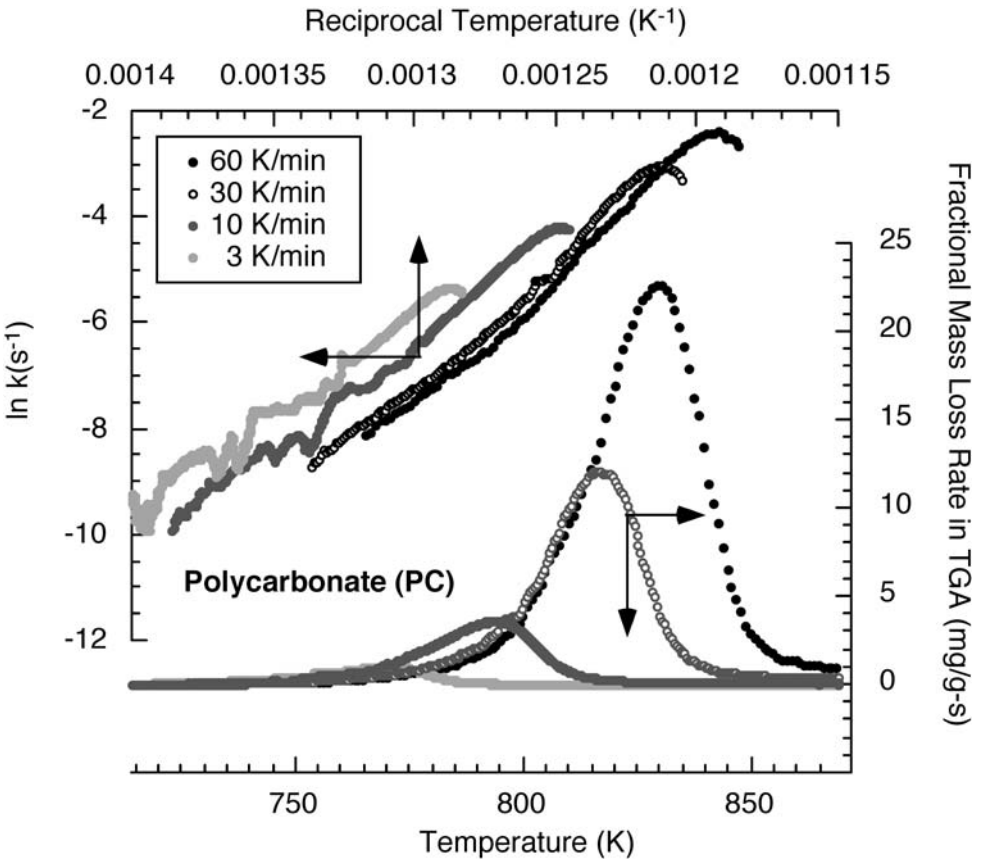

Fig. 9. Instantaneous rate plot (upper left) and original TGA data (lower right) for the char-forming polycarbonate (PC).

CONCLUSIONS

It is shown that the heating rates used in thermal analysis methods (TGA, MCC) are comparable to the heating rates at burning surfaces of polymers in fires and simple non-isothermal methods for determining kinetic parameters from a single thermogravimetric analysis experiment are presented. These methods, which are described as instantaneous rate and single-point, yield kinetic parameters that generally reproduce the fractional mass loss rate versus temperature data for polymers that thermally degrade in one or more steps via first-order processes. As with other nonisothermal analysis methods, the instantaneous rate and single-point methods are most reliable at the heating rate of interest, and for this reason do a better job of reproducing TGA data for consecutive or sequential reactions at individual heating rates than do nonisothermal methods that use multiple heating rates to provide an average A and E_a.

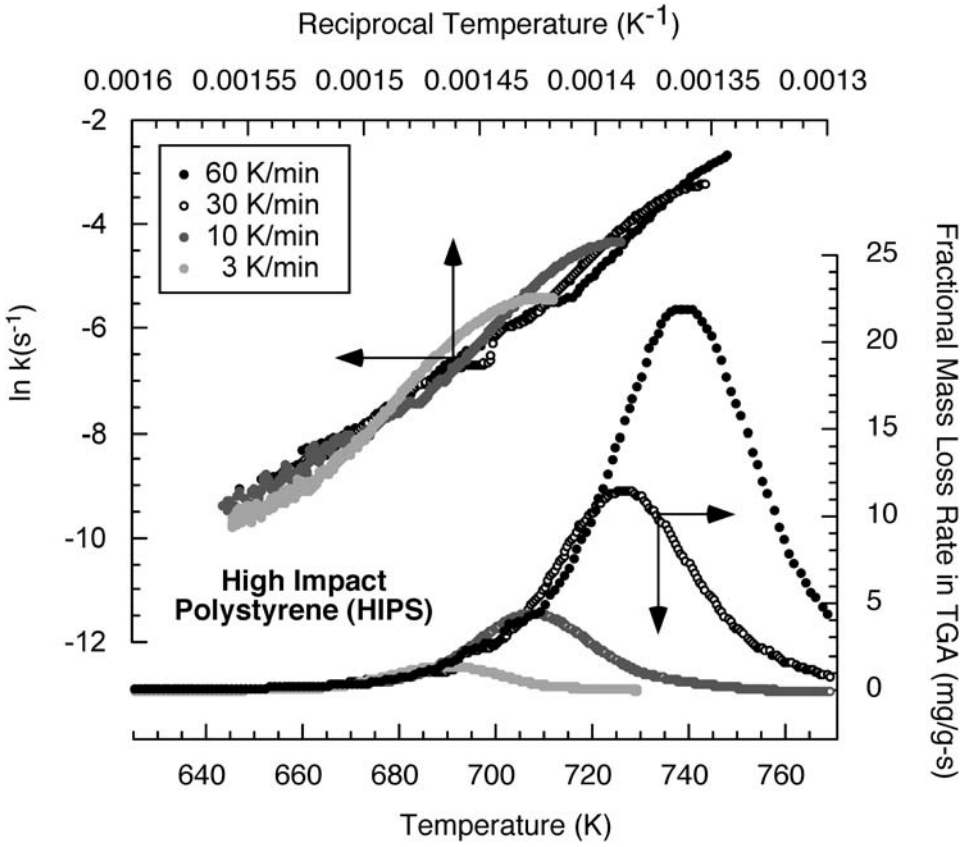

Fig. 10. Instantaneous rate plot (upper left) and original TGA data (lower right) for HIPS.

ACKNOWLEDGEMENTS

Certain commercial equipment, instruments, materials and companies are identified in this paper in order to adequately specify the experimental procedure. This in no way implies endorsement or recommendation by the Federal Aviation Administration or TAMI.

REFERENCES

[1] Vyazovkin, S., and Wight, C.A., (1997) Kinetics in Solids, Annual Review of Physical Chemistry, 48: 125-149. http://dx.doi.org/10.1146/annurev.physchem.48.1.125

[2] Staggs, J.E.J., (1997) A Theoretical Investigation into Modelling Thermal Degradation of Solids Incorporating Finite Rate Kinetics, Combustion Science and Technology, 123: 1-6. http://dx.doi.org/10.1080/00102209708935631

[3] Lyon, R.E., (2000) Heat Release Kinetics, Fire and Materials, 24(4): 179-186. http://dx.doi.org/10.1002/1099-1018(200007/08) 24:4<179::AID-FAM736>3.0.CO;2-V

[4] Lyon, R.E., (1997) An Integral Method of Nonisothermal Kinetic Analysis, Thermochimica Acta, 297: 117-124. http://dx.doi.org/10.1016/S0040-6031(97)00158-5

[5] Lyon, R.E., Walters, R.N., and Stoliarov, S.I., (2007) Thermal Analysis of Flammability, Journal of Thermal Analysis and Calorimetry, 89(2): 441-448. http://dx.doi.org/10.1007/s10973-006-8257-z

[6] Kim, S., Jang, E.S., Shin, D.H., and Lee, K.H., (2004) Using Peak Properties of DTG Curve to Estimate the Kinetic Parameters of the Pyrolysis Reaction: Application to High Density Polyethylene, Polymer Degradation and Stability, 85: 799-805. http://dx.doi.org/10.1016/j.polymdegradstab.2004.03.009

[7] Eom, Y., Kim, S., Kim, S.S., and Chung, S.H., (2006) Application of Peak Property Method for Estimating Apparent Kinetic Parameters of Cellulose Pyrolysis Reactions, Journal of Industrial Engineering Chemistry, 12(6): 846-852.

[8] Kissinger, H.E., (1957) Reaction Kinetics in Differential Thermal Analysis, Analytical Chemistry, 29(11): 1702-1706. http://dx.doi.org/10.1021/ac60131a045

[9] Lyon, R.E., Plastics and Rubber, in Handbook of Building Materials for Fire Protection, C.A. Harper, ed., McGraw-Hill, New York, Chapter 3, pp. 1-51, 2004.

[10] Stoliarov, S.I., and Lyon, R.E., Thermo-Kinetic Model of Burning, Technical Note DOT/FAA/AR-TN08/17, Federal Aviation Administration, May 2008.

[11] Standard Test Method for Heat and Visible Smoke Release Rates for Materials and Products Using and Oxygen Consumption Calorimeter, ASTM 1354, American Society for Testing & Materials International, West Conshohocken, PA.

[12] Stoliarov, S.I., Safronava, N., and Lyon, R.E., (2009) The Effect of Variation in Polymer Properties on the Rate of Burning, Fire and Materials, 33: 257-271. http://dx.doi.org/10.1002/fam.1003

[13] Stoliarov, S.I., and Walters, R.N., (2008) Determination of the Heats of Gasification of Polymers Using Differential Scanning Calorimetry, Polymer Degradation and Stability, 93: 422-427. http://dx.doi.org/10.1016/j.polymdegradstab.2007.11.022

[14] Schartel, B., and Weib, W., (2010) Temperature Inside Burning Polymer Specimens: Pyrolysis Zone and Shielding, Fire and Materials, 34(5): 217-235. http://dx.doi.org/10.1002/fam.1007